Journal of Computational and Applied Mathematics 296 (2016) 293–302

Contents lists available at ScienceDirect

Journal of Computational and Applied Mathematics

journal homepage: www.elsevier.com/locate/cam

A numerical study of the Whitham equation as a model for steady surface water waves

Handan Borluk [a], Henrik Kalisch [b], David P. Nicholls [c,*]

[a] Department of Basic Sciences, Istanbul Kemerburgaz University, Bagcilar, Turkey

[b] Department of Mathematics, University of Bergen, Postbox 7800, 5020 Bergen, Norway

[c] Department of Mathematics, Statistics, and Computer Science, University of Illinois at Chicago, Chicago, IL 60607, United States

ARTICLE INFO

Article history:
Received 12 April 2015
Received in revised form 17 August 2015

Keywords:
Whitham equation
Stokes waves
Transformed field expansions
Cosine collocation method
Numerical bifurcation analysis

ABSTRACT

The object of this article is the comparison of numerical solutions of the so-called Whitham equation to numerical approximations of solutions of the full Euler free-surface water-wave problem. The Whitham equation

$$\eta_t + \frac{3}{2}\frac{c_0}{h_0}\eta\eta_x + K_{h_0} * \eta_x = 0$$

was proposed by Whitham (1967) as an alternative to the KdV equation for the description of wave motion at the surface of a perfect fluid by simplified evolution equations, but the accuracy of this equation as a water wave model has not been investigated to date.

In order to understand whether the Whitham equation is a viable water wave model, numerical approximations of periodic solutions of the KdV and Whitham equation are compared to numerical solutions of the surface water wave problem given by the full Euler equations with free surface boundary conditions, computed by a novel Spectral Element Method technique. The bifurcation curves for these three models are compared in the phase velocity–waveheight parameter space, and wave profiles are compared for different wavelengths and waveheights. It is found that for small wavelengths, the steady Whitham waves compare more favorably to the Euler waves than the KdV waves. For larger wavelengths, the KdV waves appear to be a better approximation of the Euler waves.

1. Introduction

The KdV equation was found by Boussinesq [1] and Korteweg and de Vries [2] as a model equation whose solutions approximately describe the wave motion at the surface of a shallow fluid layer in a certain parameter range. Assuming that the undisturbed depth of the fluid is h_0, and waves with an amplitude a and a wavelength λ are to be described, the KdV equation

$$\eta_t + c_0\eta_x + \frac{3}{2}\frac{c_0}{h_0}\eta\eta_x + \frac{1}{6}c_0h_0^2\eta_{xxx} = 0, \tag{1.1}$$

has been shown to be a fair model for surface waves over intermediate time scales if the amplitude to depth ratio a/h_0 is small and comparable to the square of the depth to wavelength ratio h_0/λ. Eq. (1.1) is then valid for waves which

* Corresponding author.
E-mail addresses: borluk@gmail.com (H. Borluk), henrik.kalisch@math.uib.no (H. Kalisch), davidn@uic.edu (D.P. Nicholls).

http://dx.doi.org/10.1016/j.cam.2015.09.018
0377-0427/

travel predominantly to the right [3–6]. Note that $c_0 = \sqrt{gh_0}$ is the limiting long-wave speed, and g is the gravitational acceleration.

The linear dispersion relation in the KdV equation is found for a solution of the form $\cos(kx - \omega t)$, where $k = \frac{2\pi}{\lambda}$ is the wave number, and ω is the circular frequency. If such a function is to solve the linearized equation then the phase velocity $c(k) = \frac{\omega}{k}$ needs to satisfy the relation

$$c(k) = c_0 - \frac{1}{6}c_0 h_0^2 k^2. \tag{1.2}$$

The dispersion relation (1.2) is a second-order approximation to the dispersion relation of the linearized full surface water-wave problem

$$c(k) = \sqrt{\frac{g}{k}\tanh(kh_0)} = c_0 - \frac{1}{6}c_0 h_0^2 k^2 + \mathcal{O}(h_0^4 k^4). \tag{1.3}$$

It appears immediately that (1.2) approximates (1.3) well only for very small k, i.e. for waves of rather large wavelength. Since the linear phase speed of shorter waves is not described accurately by the KdV equation, one may envision an alternative nonlinear model equation which incorporates an exact description of the linear dispersion relation. To this end, we define the kernel K_{h_0} by

$$K_{h_0} := \mathcal{F}^{-1}\left(\sqrt{\frac{g\tanh(h_0\xi)}{\xi}}\right),$$

where the inverse Fourier transform $\mathcal{F}^{-1}$ is given by

$$f(x) = \left(\mathcal{F}^{-1}F\right)(x) := \frac{1}{2\pi}\int_{-\infty}^{\infty} F(\xi)e^{ix\xi}\,d\xi.$$

The alternative model for surface waves which may have shorter wavelength which was put forward by Whitham [7] then takes the form

$$\eta_t + \frac{3}{2}\frac{c_0}{h_0}\eta\eta_x + K_{h_0} * \eta_x = 0. \tag{1.4}$$

The rationale behind this model is that the dispersion relation of the linearized Whitham equation is the same as the exact dispersion relation (1.3) of the full water-wave problem, and the nonlinear term is of the same form as in the KdV equation. Hence, it is expected that the Whitham equation will be able to model more accurately waves of shorter wavelength. However, to the best of our knowledge, a verification of the modeling properties of the Whitham equation does not currently exist in the literature.

In the present contribution, we will take up this question in the context of steady periodic wave patterns. Taking numerical approximations of solutions of the Euler equations as the basis for the comparison, we compute numerical solutions of the Whitham and KdV equations, and compare them to the Euler solutions. As it will turn out, at least in the context of steady periodic wave patterns, the Whitham equation is indeed able to provide approximations of shorter waves with greater accuracy than the KdV equation.

In order to find traveling wave solutions of the full water-wave problem, we use a modification of the numerical method devised by one of the authors and F. Reitich [8,9]. This method is based upon boundary perturbations where the parameter is the wave slope/height. Within the disk of analyticity of the relevant Taylor series (of the surface deformation and velocity potential), this algorithm delivers highly accurate traveling water wave solutions at *any* point along the bifurcation branch in a robust and high-order fashion. These "Transformed Field Expansion" (TFE) recursions can be proven to be strongly convergent in an appropriate Sobolev space [8], and the resulting numerical algorithm demonstrated to be consistent and stable [10]. Simply put, the method is essentially Stokes' approach *preceded* by a domain-flattening change of variables which, remarkably, delivers a stable, accurate, and provably convergent algorithm [9]. The novel aspect of the approach advocated here is the utilization of a Legendre Spectral Element Method (SEM) for depth discretization in place of the standard Chebyshev tau approach put forward in [9,11]. As discussed in previous work by one of the authors [12] on the related problem of simulating Dirichlet–Neumann Operators, this methodology provides greater flexibility with its possibilities for both h- and p-refinement.

While the Whitham equation has been known as a phenomenological model for surface waves for several decades, formal asymptotic and mathematically rigorous derivations of the Whitham equation as an asymptotic water wave model appear only in the very recent literature [13,14]. In particular, this means that it is difficult in the context of the Whitham equation to understand the flow below a given wave pattern at the surface. In principle, in a steady periodic flow without critical layers, it is possible to determine the velocity field from the shape of the free surface if it is known exactly [15]. In the case of the KdV equation, one may find the velocity field below a given surface wave pattern [16], and it is also possible to reconstruct the pressure [17] to the same order of approximation as the model equation is valid. Such developments do not have a counterpart in the context of the Whitham equation.

On the other hand, it appears that the Whitham equation does feature some pertinent properties of the surface water wave problem. For instance, the Whitham equation possesses solitary-wave solutions [18], and traveling-wave solutions

[19,20], and the periodic traveling-wave solutions exhibit modulational instability in a similar way as periodic solutions of the full water wave problem [21,22]. One particular question which was already considered by Whitham is whether (1.4) admits breaking and peaking waves. While there are plenty of works concerning mathematical properties of the Whitham and related equations [23–26], the questions of wave breaking and peaking have not been answered conclusively. Numerical work indicates that there is a highest wave which has a derivative singularity, but to investigate these questions in more detail might require more specialized numerical tools such as the method put forward in [27].

2. Formulation of the problem

Consider an incompressible and inviscid fluid running in a narrow open channel. Suppose that transverse effects can be neglected. The free-surface problem can then be studied in the (x, z)-plane, and the governing equations are the Euler momentum equations

$$\begin{aligned} u_t + uu_x + wu_z &= -\frac{p_x}{\rho} && \text{in } 0 < z < h_0 + \eta(x,t), \\ w_t + uw_x + ww_z &= -\frac{p_z}{\rho} - g && \text{in } 0 < z < h_0 + \eta(x,t), \end{aligned}$$

where $p(x, z, t)$ denotes the pressure at a point (x, z) and a time t, $\eta(x, t)$ is the excursion of the free surface from its rest position, and $u(x, z, t)$ and $w(x, z, t)$ are the horizontal and vertical velocities, respectively. These equations are supplemented with the continuity equation and irrotationality condition, which are

$$\begin{aligned} u_x + w_z &= 0, && \text{in } 0 < z < h_0 + \eta(x,t), \\ w_x - u_z &= 0, && \text{in } 0 < z < h_0 + \eta(x,t). \end{aligned}$$

The equations can be studied on an infinite domain $-\infty < x < \infty$, and in particular with periodic boundary conditions. The bottom boundary condition is given by the requirement that the fluid cannot penetrate the bottom which is expressed mathematically as

$$w = 0, \qquad \text{at } z = 0.$$

The surface boundary conditions are the kinematic condition

$$\eta_t + u\eta_x = w, \quad \text{on } z = h_0 + \eta(x,t),$$

and the dynamic condition

$$p = 0, \quad \text{on } z = h_0 + \eta(x,t).$$

This formulation of the free surface problem is well known, and a derivation of the Euler equation as well as the boundary conditions may be found for instance in [28]. We introduce the standard non-dimensional variables

$$x \to h_0 x, \qquad \eta \to h_0 \eta, \qquad t \to \frac{h_0}{c_0} t, \qquad z \to h_0 z, \qquad u \to c_0 u, \qquad v \to c_0 v, \qquad p \to \rho c_0^2 p. \tag{2.1}$$

The Euler equations and the corresponding side conditions may be written as

$$\begin{aligned} u_t + uu_x + wu_z &= -p_x, \\ w_t + uw_x + ww_z &= -p_z - 1, \end{aligned} \tag{2.2}$$

$$u_x + w_z = 0 \quad \text{and} \quad u_z - w_x = 0. \tag{2.3}$$

$$p = 0 \quad \text{and} \quad \eta_t + u\eta_x = w, \quad \text{at } z = 1 + \eta(x,t). \tag{2.4}$$

The steady problem to be solved is as follows: Since we assume irrotational flow, a velocity potential ϕ can be used. This potential is characterized by the relation $(u, w) = \nabla\phi$. Assuming steady waves with translational velocity c, so that $\phi(x, z, t) = \Phi(x - ct, z)$ and $\eta(x, t) = E(x - ct)$, yields the following set of governing equations and boundary conditions for E and ϕ:

$$\Phi_{xx} + \Phi_{zz} = 0 \quad \text{in } 0 < z < 1 + E(x). \tag{2.5}$$

$$-cE_x + \Phi_x E_x + \Phi_z = 0, \quad \text{on } z = 1 + E(x), \tag{2.6}$$

$$-c\Phi_x + \frac{1}{2}\Phi_x^2 + \frac{1}{2}\Phi_z^2 - E = 0, \quad \text{on } z = 1 + E(x), \tag{2.7}$$

$$\Phi_z = 0, \quad \text{on } z = 0. \tag{2.8}$$

Solutions of this problem will be found using a numerical bifurcation analysis. For a given wavelength (and disallowing subharmonic bifurcations), the problem above is linearized, and it is clear that the linear problem has a solution for every $c \in \mathbb{R}$. However, for one particular value c^* of c, the linearized problem is given in terms of a singular operator, and at that

point, a branch of solutions of the nonlinear problem may be found. Some aspects of this procedure are explained in [29], and in particular, it turns out that c^* is determined by the dispersion relation. For a given wavelength $\lambda = 2\pi/k$ we have

$$c^* = \sqrt{\frac{g}{k}\tanh(kh_0)}.$$

3. Numerical approximation of Euler equations

For the details of the numerical procedure we utilize to simulate solutions to (2.5), (2.6), (2.7), and (2.8) we refer the interested reader to [8,9] and indicate below our new enhancements. To summarize these developments we outline the following crucial elements. We begin with the change of variables

$$x' = x, \qquad z' = h\left(\frac{z-\eta}{h+\eta}\right)$$

which are σ-coordinates in atmospheric science [30] and the C-method in electromagnetics [31]. The transformed velocity potential

$$U(x', z') = \Phi(x', (h+\eta)z'/h + \eta)$$

and surface deformation satisfy inhomogeneous versions of (2.5), (2.6), (2.7), and (2.8) which are specified in detail in [8,9]. Due to their particular form, solutions to these equations in the forms of regular perturbation expansion of the unknowns, $\{c, \eta, u\}$, namely

$$\{c, E, U\} = \{c(\varepsilon), E(x';\varepsilon), U(x', z';\varepsilon)\} = \sum_{n=0}^{\infty}\{c_n, E_n(x'), U_n(x', z')\}\varepsilon^n,$$

are natural and, as shown in [8], strongly convergent. We approximate the quantities $\{c, E, U\}$ with truncations of these Taylor series

$$\{c, E, U\} \approx \{c^N, E^N, U^N\} := \sum_{n=0}^{N}\{c_n, E_n(x'), U_n(x', z')\}\varepsilon^n.$$

Assuming 2π periodicity, we pose Fourier approximations to both E^N

$$E^N \approx E^{N,N_x} := \sum_{n=0}^{N}\sum_{k=-N_x/2}^{N_x/2-1}\hat{E}_{n,k}e^{ikx'}\varepsilon^n,$$

and U^N

$$U^N \approx U^{N,N_x} := \sum_{n=0}^{N}\sum_{k=-N_x/2}^{N_x/2-1}\hat{U}_{n,k}(z')e^{ikx'}\varepsilon^n.$$

In [9] we advocated a Chebyshev approximation to $\hat{U}_{n,k}(z')$ in the depth variable, z',

$$\hat{U}_{n,k} \approx \hat{U}_{n,k}^{N_z,\mathrm{Cheby}} := \sum_{\ell=0}^{N_z}\hat{U}_{n,k,\ell}^{\mathrm{Cheby}}T_\ell\big((2z'-h)/h\big)$$

where T_ℓ is the ℓ-th Chebyshev polynomial. By enforcing the transformed equations at the appropriate collocation points one can realize a spectrally accurate Fourier, Chebyshev, Taylor approach to the problem of approximating solutions of the traveling water wave problem whose utility has been studied in detail in the work [9].

However, the *global* nature of the basis functions is a weakness. While the choice of a Chebyshev basis ensures efficiency, as the domain size increases N_z must increase. This was noted and investigated by one of the authors in [12] in the context of the computation of Dirichlet–Neumann Operators. It was concluded that a Legendre Spectral Element Method (SEM) was a compelling alternative and thus we now describe a novel approach to computing traveling water waves via this algorithm.

As described in [32], the SEM has features of both *h*-and *p*-Finite Element Methods (FEMs). More specifically the domain is partitioned into elements

$$[-h, 0] = \bigcup_{e=1}^{N_E}[a_e, b_e].$$

Lagrangian interpolation formulas are used on each element, and basis functions have local support. From the point of view of *p*-refinement, high-order polynomials are used as basis functions (to deliver high accuracy for smooth solutions). However, SEM have the additional feature that Gaussian quadrature is used to deliver sparsity from both the local support of the basis functions and the integration rules used.

In brief, the relevant two-point boundary value problem for $\hat{U}_{n,k}(z')$, see [8,9], is posed weakly with the Dirichlet condition (at the surface $z' = 0$) enforced essentially and the Robin condition (at the bottom $z' = -h$) imposed naturally. The elements

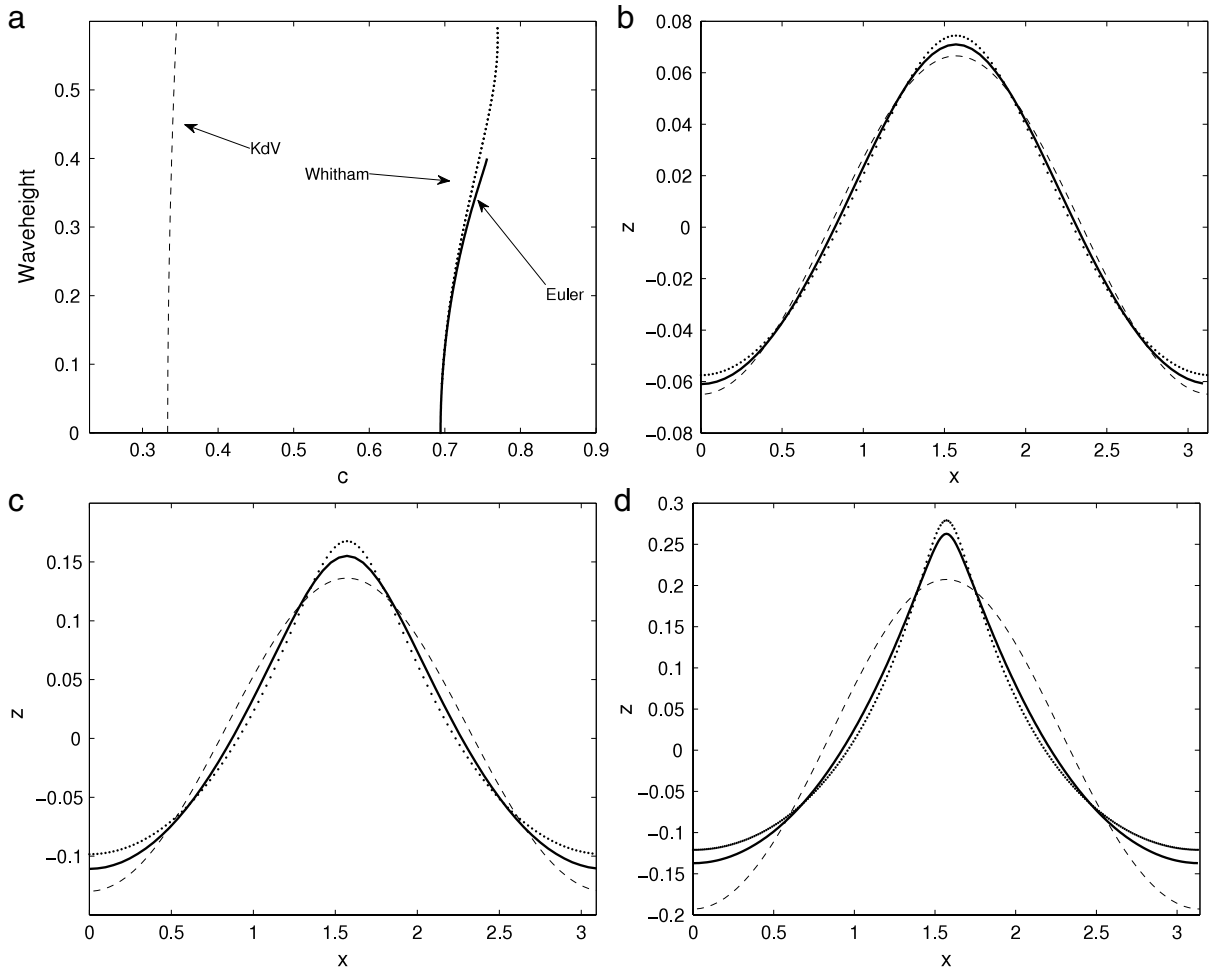

Fig. 1. Wavelength $\lambda = \pi$: In panel (a) bifurcation diagrams for the Euler (thick solid), Whitham (dotted) and KdV (dashed) equations are shown for wavelength π. In panel (b), three waves with waveheight 0.131 are shown. The corresponding phase velocities are $c = 0.713$ for the Euler approximation, $c = 0.701$ for the Whitham wave, and $c = 0.334$ for the KdV wave. In panel (c), three waves with waveheight 0.266 are shown. The corresponding phase velocities are $c = 0.7326$ for the Euler approximation, $c = 0.7190$ for the Whitham wave, and $c = 0.336$ for the KdV wave. In panel (d), three waves with waveheight 0.400 are shown. The corresponding phase velocities are $c = 0.765$ for the Euler approximation, $c = 0.746$ for the Whitham wave, and $c = 0.339$ for the KdV wave. The waves all have zero mean.

$[a_e, b_e]$ are mapped to the reference element $[-1, 1]$ and the approximate solution on element e is expanded in Lagrange interpolatory polynomials, $\pi_\ell(s)$, based upon the Gauss–Lobatto–Legendre (GLL) points

$$\hat{U}^e_{n,k} \approx \hat{U}^{e,N_z}_{n,k} := \sum_{\ell=0}^{N_z} \hat{U}^e_{n,k,\ell}\pi_\ell(s), \quad s \in [-1, 1].$$

Local mass and stiffness matrices are assimilated into their global counterparts via standard FEM technology. These SEM methods have many advantages for differential equations with smooth solutions including high-order accuracy and adaptive refinement in both polynomial order (p-refinement) and spatial discretization (h-refinement).

Numerical bifurcation branches of steady solutions of the full surface water wave problem with various wavelengths are shown in panel (a) of Figs. 1–3. Solution profiles with different amplitudes are shown in panels (b), (c) and (d) of these figures.

4. Bifurcation for Whitham and KdV waves

Introducing the same non-dimensional variables as in Section 2, and defining the kernel K by

$$K = \mathcal{F}^{-1}\left(\sqrt{\frac{\tanh(\xi)}{\xi}}\right), \tag{4.1}$$

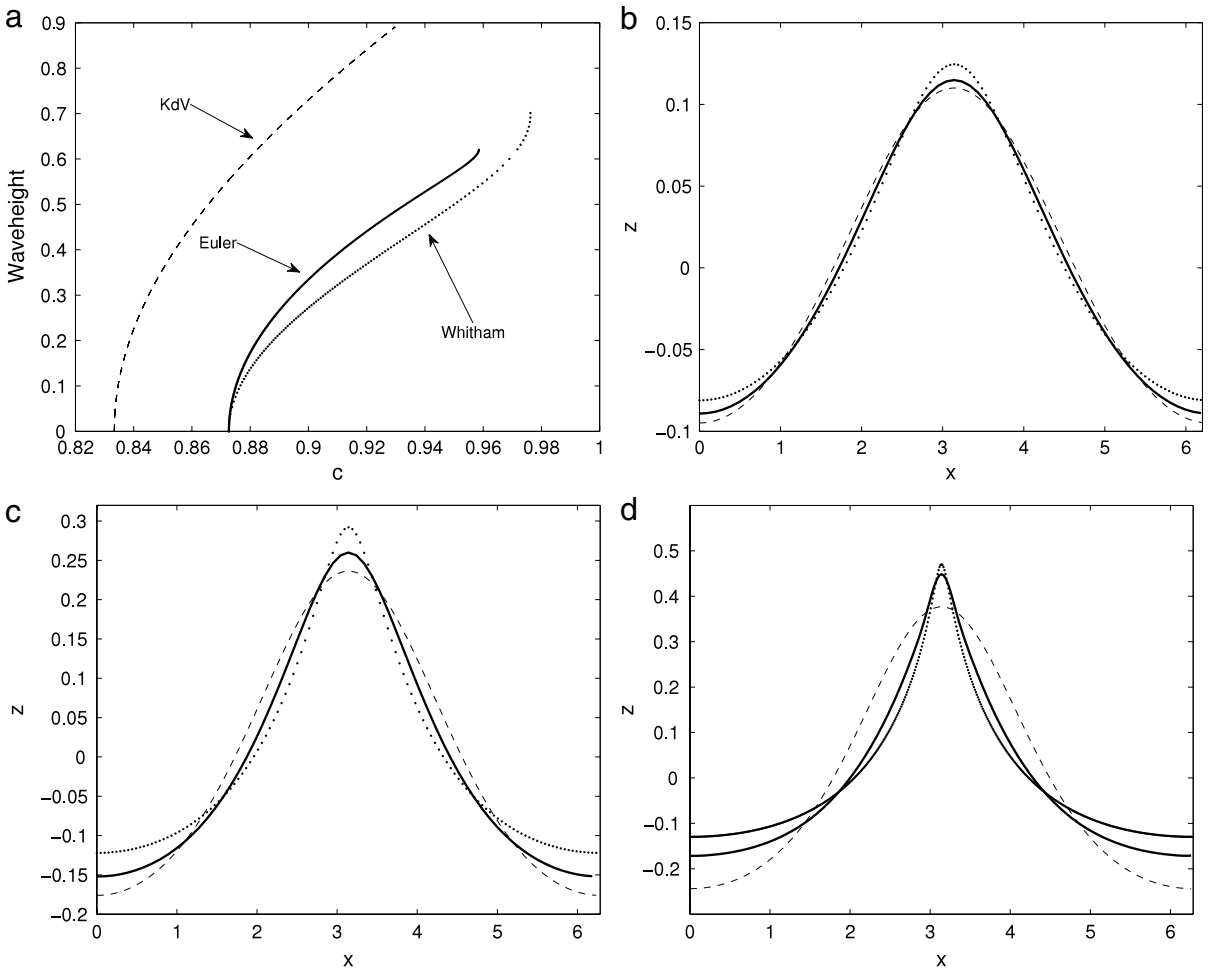

Fig. 2. Wavelength $\lambda = 2\pi$: In panel (a) bifurcation diagrams for the Euler (thick solid), Whitham (dotted) and KdV (dashed) equations are shown for wavelength 2π. In panel (b), three waves with waveheight 0.204 are shown. The corresponding phase velocities are $c = 0.883$ for the Euler approximation, $c = 0.889$ for the Whitham wave, and $c = 0.806$ for the KdV wave. In panel (c), three waves with waveheight 0.412 are shown. The corresponding phase velocities are $c = 0.914$ for the Euler approximation, $c = 0.930$ for the Whitham wave, and $c = 0.856$ for the KdV wave. In panel (d), three waves with waveheight 0.620 are shown. The corresponding phase velocities are $c = 0.960$ for the Euler approximation, $c = 0.973$ for the Whitham wave, and $c = 0.883$ for the KdV wave. The waves all have zero mean.

Eqs. (1.1) and (1.4) become

$$\eta_t + \eta_x + \frac{3}{2}\eta\eta_x + \frac{1}{6}\eta_{xxx} = 0 \tag{4.2}$$

and

$$\eta_t + \frac{3}{2}\eta\eta_x + K * \eta_x = 0. \tag{4.3}$$

Traveling-wave solutions are sought in the form $\eta(x, t) = E(x - ct)$, and after an integration, the equations transform into

$$-cE + E + \frac{3}{4}E^2 + \frac{1}{6}E_{xx} = 0 \tag{4.4}$$

and

$$-cE + \frac{3}{4}E^2 + K * E = 0. \tag{4.5}$$

It is a general fact (see e.g. [19]) that the Fourier multiplier for periodic solutions is the same as for solutions on the real line. Writing the linearized equations (4.4) and (4.5) in Fourier variables reveals that the bifurcation points depend on the

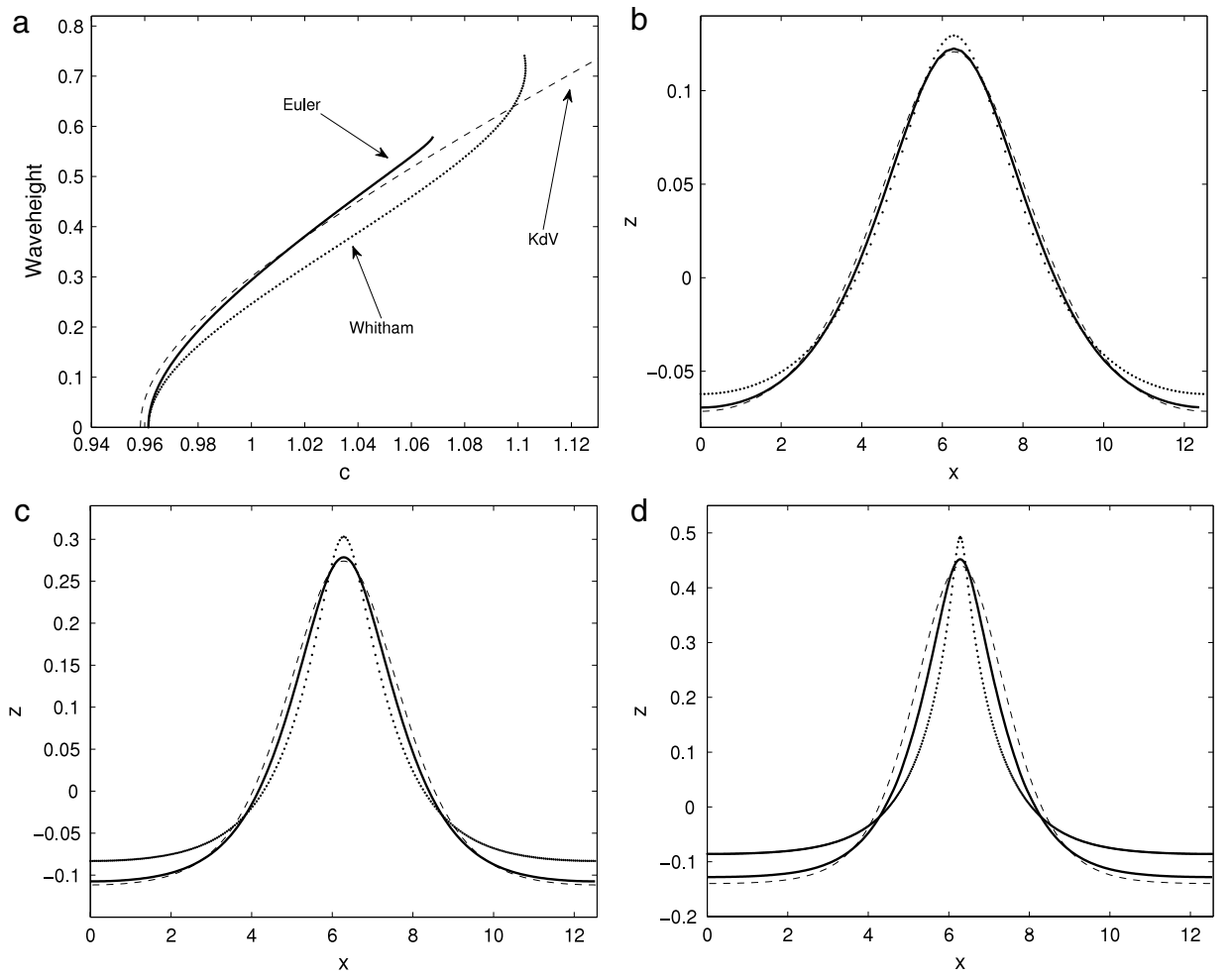

Fig. 3. Wavelength $\lambda = 4\pi$: In panel (a) bifurcation diagrams for the Euler (thick solid), Whitham (dotted) and KdV (dashed) equations are shown for wavelength 4π. In panel (b), three waves with waveheight 0.192 are shown. The corresponding phase velocities are $c = 0.9800$ for the Euler approximation, $c = 0.9865$ for the Whitham wave, and $c = 0.9770$ for the KdV wave. In panel (c), three waves with waveheight 0.3852 are shown. The corresponding phase velocities are $c = 1.0213$ for the Euler approximation, $c = 1.0390$ for the Whitham wave, and $c = 1.0219$ for the KdV wave. In panel (d), three waves with waveheight 0.5799 are shown. The corresponding phase velocities are $c = 1.068$ for the Euler approximation, $c = 1.088$ for the Whitham wave, and $c = 1.0793$ for the KdV wave. The waves all have zero mean.

wavelength $\lambda = 2\pi/k$. Indeed, the bifurcation points are given by the expressions (1.3) and (1.2) of the dispersion relation, so that

$$c^*_{\text{Whitham}} = \sqrt{\frac{1}{k}\tanh k},$$

and

$$c^*_{\text{KdV}} = 1 - \frac{1}{6}k^2.$$

Solutions of (4.4) are given by the well known cnoidal functions, such as explained in [33] for instance. On the other hand, for the comparison of the bifurcation curves it is actually more convenient to use a numerical bifurcation method to solve both the Whitham and the KdV equation.

5. Numerical approximation of Whitham and KdV waves

Solutions of (4.5) are approximated using a spectral cosine collocation method [34,35]. For the use of spectral methods, it is convenient to rescale Eq. (4.5) to the interval $[0, 2\pi]$. This rescaling can be achieved by defining $E(x) \to E(ax)$, where $a = \frac{\lambda}{2\pi}$. Special attention has to be paid to the operator K_{h_0}. A straightforward calculation shows that

$$\big(K_{h_0} * f\big)(ax) = \sqrt{a} K_{h_0/a} * \big(f(a\,\cdot)\big)(x). \tag{5.1}$$

Therefore, the rescaled equation for 2π-periodic solutions in non-dimensional form is

$$-c\,E+\frac{3}{4}E^2+\sqrt{a}K_{1/a}*E=0. \tag{5.2}$$

To simplify the problem, we assume that solutions are even, so that a cosine method can be used. To define the cosine-collocation projection of (5.2), first define the subspace

$$S_N=\operatorname{span}_{\mathbb{R}}\left\{\cos(lx)\;\middle|\;0\le l\le N-1\right\}$$

of $L^2(0,\pi)$, and the collocation points $x_n=\pi\frac{2n-1}{2N}$ for $n=1,\dots,N$. The discretization is defined by seeking E_N in S_N satisfying the equation

$$-cE_N+\frac{3}{4}E_N^2+\sqrt{a}K_{1/a}^N E_N=0, \tag{5.3}$$

where the operator $K_{1/a}^N$ is the discrete form of $K_{1/a}$ defined in (4.1). The discrete cosine representation of E_N given by

$$E_N(x)=\sum_{l=0}^{N-1}w(l)\hat{E}_N(l)\cos(lx),$$

where

$$w(l)=\begin{cases}\sqrt{1/N}, & l=0,\\ \sqrt{2/N}, & l\ge 1,\end{cases}$$

and $\hat{E}_N(l)$ are the discrete cosine coefficients, given by

$$\hat{E}_N(l)=w(l)\sum_{n=1}^{N}E_N(x_n)\cos(lx_n),\quad \text{for } l=0,\dots,N-1.$$

Now if Eq. (5.3) is enforced at the collocation points x_n, the term $K^N E_N$ may be practically evaluated with the help of the matrix $\left[K_{1/a}^N\right](m,n)$ by

$$\left[K_{1/a}^N\right]E_N(x_m)=\sum_{n=1}^{N}\left[K_{1/a}^N\right](m,n)E_N(x_n),$$

where the matrix $\left[K_{1/a}^N\right](m,n)$ is defined by

$$\left[K_{1/a}^N\right](m,n)=\sum_{l=0}^{N-1}w^2(l)\sqrt{\frac{1}{l}\tanh(l/a)}\;\cos(lx_n)\cos(lx_m).$$

Thus, Eq. (5.3) enforced at the collocation points x_n yields a system of N nonlinear equations, which can be solved using Newton's method. The cosine expansion removes the singularities of the Jacobian matrix due to translational invariance and symmetry of the solutions. The wave velocity c is used as the bifurcation parameter, but as the turning point is approached, it is more convenient to change to a waveheight parametrization. The computation can be started for c close to but smaller than the critical speed $c^*_{\text{Whitham}}=\sqrt{\frac{\tanh(k)}{k}}$. The initial guess for the first computation can be given by a cosine function, or using the Stokes expansions given in the Appendix. Since Eq. (5.3) is based on setting the constant of integration to zero, one needs to use a Galilean transformation in order to find a solution which has mean zero, and can be compared to solutions of the full Euler equation. The Galilean shift is explained in [19].

The computations of the numerical bifurcation branch for the KdV equation proceeds along the same lines as laid down above for the Whitham equation. The scaled discrete equation is

$$-c\,E_N+E_N+\frac{3}{4}E_N^2+\frac{1}{a^2}\partial_x^2E_N=0, \tag{5.4}$$

and the collocation matrix for the second derivative operator can be computed as

$$\left[\partial_x^2\right](m,n)=\sum_{l=0}^{N-1}w^2(l)(-l^2)\;\cos(lx_n)\cos(lx_m).$$

Numerical bifurcation branches of steady Whitham and KdV solutions are shown in panels (a) of Figs. 1–3, where they are compared to the bifurcation branches of steady solutions of the full Euler equations.

6. Discussion of numerical results

We now present the results of a number of computations, in which the solutions of the full water-wave problem are compared with the corresponding solutions of the two model equations in view in this paper.

Fig. 1 shows the case where the wavelength is set to $\lambda = \pi$. In this case, the normalized depth to wavelength ratio is $1/\pi \sim 0.32$. We see in panel (a) that the bifurcation points for the Euler and Whitham branches coincide. This is because the linear dispersion relation is the same for these two models. Moreover, both Whitham and Euler branches are finite, while the KdV branch is infinite. The shape of all three waves is similar for small amplitudes, such as shown in panel (b) for waveheight 0.131. However, as already visible in panel (a), the Whitham wave and the Euler wave have similar wave speeds whilst the wavespeed of the KdV wave is only about half of the value of the Euler solution. This is a remnant of the fact that the linear dispersion relation (1.2) of the KdV equation does not give a faithful representation of the dispersion relation (1.3).

For larger waveheights, the Whitham wave is situated a bit higher, while the KdV wave is situated a bit lower than the Euler solution (panel (c)). Note again that we have arranged the waves so as to have mean value zero. A comparison of the profiles in which the crests are aligned would yield different, and apparently closer comparisons. Finally in panel (d), we compare the highest wave achieved with the Euler code to Whitham and KdV waves of the same waveheight. Here, it appears that the Whitham wave is a bit narrower and with a sharper peak than the Euler wave, but it resembles the shape of the Euler solution more closely than the KdV wave does.

Fig. 2 shows the case where the wavelength is set to $\lambda = 2\pi$. In this case, the normalized depth to wavelength ratio is $1/2\pi \sim 0.16$. As in the previous figure, the bifurcation points for the Euler and Whitham branches coincide, and both Whitham and Euler branches are finite, while the KdV branch is infinite. On the other hand, the waveshape of the KdV wave is somewhat closer to the Euler approximation than the Whitham wave for small waveheights (panel (b)). For larger waveheights, the Whitham wave is situated a bit higher, while the KdV wave is situated a bit lower than the Euler solution (panel (c)). Note again that we have arranged the waves so as to have mean value zero. Finally in panel (d), we compare the highest wave achieved with the Euler code to Whitham and KdV waves of the same waveheight. Here, it appears that the Whitham wave resembles the shape of the Euler solution more closely than the KdV wave does.

Fig. 3 shows the case where the wavelength is fixed to be $\lambda = 4\pi$. In this case, the normalized depth to wavelength ratio is $1/4\pi \sim 0.08$. We see in panel (a) that the bifurcation points for the Euler and Whitham branches coincide, and that the KdV bifurcation point is also very close to the other two bifurcation points. Again, both Whitham and Euler branches are finite, while the KdV branch is infinite. In the case of longer wavelengths, such as $\lambda = 4\pi$ shown here, the KdV wave appears to be a better approximation of the Euler wave both for smaller and larger amplitudes.

7. Conclusion

Simulation properties of the Whitham equation as a model for waves at the surface of a body of fluid have been investigated. It has been found that periodic traveling-wave solutions of the Whitham equation are good approximations to solutions of the full free-surface water wave problem. Since the derivations of the model equations such as KdV equation are based on the inviscid problem, the Euler equations have been used as the basis for the comparison.

A comparison of high-order numerical approximations of solutions of the Euler equations with spectral cosine collocation approximations of the KdV and Whitham equations gave the following findings. The bifurcation branches for both the Euler equations and the Whitham equation are finite, while the bifurcation branch for the KdV equation is infinite. In general, the Whitham waves are always a little narrower and taller than the Euler waves, while the corresponding KdV waves are somewhat wider than the Euler solutions. For waves of shorter wavelength, the Whitham equation appears to provide a closer approximation of the Euler waves than the KdV equation does. Both the phase velocity and the shape of traveling waves of wavelength shorter than 2π are faithfully described by the Whitham equation. For larger wavelength, the KdV equation is a better model, and this is in line with the known validity of the KdV equation as a long wave model.

Appendix. Stokes approximation

In order to double check the curves computed with the numerical bifurcation algorithm, it is convenient to use asymptotic formulae for the approximation of periodic traveling waves of these equations. This approach was originally used by Stokes for the computation of approximate solutions of the full water wave problem, and the approximate solutions are therefore often called Stokes waves. Using this approach which is also recounted in [33], the Stokes waves for Whitham equation can be written as

$$E = \varepsilon \cos(kx) + \varepsilon^2 A \cos(2kx) + \varepsilon^3 B \cos(3kx) + \cdots,$$
$$c = \frac{\omega}{k} = \sqrt{(1/k)\tanh(k)} + \varepsilon^2 \frac{3}{4} Ak + \cdots$$

where

$$A = \frac{3}{4} \frac{3k}{2\sqrt{(1/k)\tanh(k)} - \sqrt{(2/k)\tanh(2k)}},$$

and

$$B = \frac{9}{4}\,\frac{Ak}{3\sqrt{(1/k)\tanh(k)} - \sqrt{(3/k)\tanh(2k)}}.$$

Similar formulae are derived for the KdV equation in [33]. Numerical validation of these formulae with the curves shown in Figs. 1(a), 2(a) and 3(a) shows good agreement for small amplitude waves.

References

[1] J. Boussinesq, Théorie des ondes et des remous qui se propagent le long d'un canal rectangulaire horizontal, en communiquant au liquide contenu dans ce canal des vitesses sensiblement pareilles de la surface au fond, J. Math. Pures Appl. 17 (1872) 55–108.
[2] D.J. Korteweg, G. deVries, On the change of form of long waves advancing in a rectangular channel and on a new type of long stationary wave, Phil. Mag. 39 (1895) 422–443.
[3] J.L. Bona, T. Colin, D. Lannes, Long wave approximations for water waves, Arch. Ration. Mech. Anal. 178 (2005) 373–410.
[4] W. Craig, An existence theory for water waves and the Boussinesq and Korteweg–de Vries scaling limits, Comm. Partial Differential Equations 10 (1985) 787–1003.
[5] G. Schneider, C.E. Wayne, The long-wave limit for the water wave problem. I. The case of zero surface tension, Comm. Pure Appl. Math. 53 (2000) 1475–1535.
[6] J.L. Bona, R. Smith, The initial-value problem for the Korteweg–deVries equation, Philos. Trans. R. Soc. Lond. Ser. A 278 (1975) 555–601.
[7] G.B. Whitham, Variational methods and applications to water waves, Proc. R. Soc. A 299 (1967) 6–25.
[8] D.P. Nicholls, F. Reitich, On analyticity of traveling water waves, Proc. R. Soc. Lond. Ser. A 461 (2005) 1283–1309.
[9] D.P. Nicholls, F. Reitich, Stable, high-order computation of traveling water waves in three dimensions, Eur. J. Mech. B Fluids 25 (2006) 406–424.
[10] D.P. Nicholls, J. Shen, A rigorous numerical analysis of the transformed field expnsion method, SIAM J. Numer. Anal. 47 (2009) 2708–2734.
[11] D.P. Nicholls, F. Reitich, Stability of high-order perturbative methods for the computation of Dirichlet–Neumann operators, J. Comput. Phys. 170 (2001) 276–298.
[12] D.P. Nicholls, Efficient enforcement of far-field boundary conditions in the transformed field expansions method, J. Comput. Phys. 230 (2011) 8290–8303.
[13] D. Lannes, J.-C. Saut, Remarks on the full dispersion Kadomtsev–Petviashvli equation, Kinet. Relat. Models 6 (2013) 989–1009.
[14] D. Moldabayev, H. Kalisch, D. Dutykh, The Whitham Equation as a model for surface water waves, Phys. D 309 (2015) 99–107.
[15] H. Kalisch, A uniqueness result for periodic traveling waves in water of finite depth, Nonlinear Anal. 58 (2004) 779–785.
[16] H. Borluk, H. Kalisch, Particle dynamics in the KdV approximation, Wave Motion 49 (2012) 691–709.
[17] A. Ali, H. Kalisch, Reconstruction of the pressure in long-wave models with constant vorticity, Eur. J. Mech. B Fluids 37 (2013) 187–194.
[18] M. Ehrnström, M.D. Groves, E. Wahlén, Solitary waves of the Whitham equation—a variational approach to a class of nonlocal evolution equations and existence of solitary waves of the Whitham equation, Nonlinearity 25 (2012) 2903–2936.
[19] M. Ehrnström, H. Kalisch, Traveling waves for the Whitham equation, Differential Integral Equations 22 (2009) 1193–1210.
[20] M. Ehrnström, H. Kalisch, Global Bifurcation for the Whitham equation, Math. Model. Nat. Phenom. 8 (05) (2013) 13–30.
[21] V. Hur, M. Johnson, Modulational instability in the Whitham equation for water waves, Stud. Appl. Math. 134 (2015) 120–143.
[22] N. Sanford, K. Kodama, J.D. Carter, H. Kalisch, Stability of traveling wave solutions to the Whitham equation, Physics Lett. A 378 (2014) 2100–2107.
[23] P.I. Naumkin, I.A. Shishmarev, Nonlinear Nonlocal Equations in the Theory of Waves, in: Translations of Mathematical Monographs, vol. 133, American Mathematical Society, Providence, RI, 1994.
[24] S.A. Gabov, On Whitham's equation, Dokl. Akad. Nauk SSSR 242 (1978) 993–996.
[25] C. Klein, J.-C. Saut, A numerical approach to blow-up issues for dispersive perturbations of Burgers' equation, Physica D 295 (2015) 46–65.
[26] A.A. Zaitsev, Stationary Whitham waves and their dispersion relation, Dokl. Akad. Nauk SSSR 286 (1986) 1364–1369.
[27] J.P. Boyd, A Legendre-pseudospectral method for computing travelling waves with corners (slope discontinuities) in one space dimension with application to Whitham's equation family, J. Comput. Phys. 189 (2003) 98–110.
[28] J.J. Stoker, Water Waves: The Mathematical Theory with Applications, in: Pure and Applied Mathematics, vol. 4, Interscience Publishers, New York, 1957.
[29] D.P. Nicholls, Traveling water waves: spectral continuation methods with parallel implementation, J. Comput. Phys. 143 (1998) 224–240.
[30] N.A. Phillips, A coordinate system having some special advantages for numerical forecasting, J. Atmospheric Sci. 14 (1957) 184–185.
[31] J. Chandezon, D. Maystre, G. Raoult, A new theoretical method for diffraction gratings and its numerical application, J. Opt. 11 (1980) 235–241.
[32] M.O. Deville, P.F. Fischer, E.H. Mund, High-order Methods for Incompressible Fluid Flow, in: Cambridge Monographs on Applied and Computational Mathematics, vol. 9, Cambridge University Press, Cambridge, 2002.
[33] G.B. Whitham, Linear and Nonlinear Waves, Wiley, New York, 1974.
[34] J.P. Boyd, Chebyshev and Fourier Spectral Methods, Dover Publications Inc., Mineola, 2001.
[35] D. Gottlieb, S.A. Orszag, Numerical Analysis of Spectral Methods: Theory and Applications, in: CBMS-NSF Regional Conference Series in Applied Mathematics, vol. 26, Society for Industrial and Applied Mathematics, Philadelphia, 1977.